







# Functional interplay of Epstein-Barr virus oncoproteins in a mouse model of B cell lymphomagenesis

Thomas Sommermann<sup>a,1</sup> , Tomoharu Yasuda<sup>a,2</sup>, Jonathan Ronen<sup>b,2</sup> , Tristan Wirtz<sup>a</sup>, Timm Weber<sup>a</sup> , Ulrike Sack<sup>a</sup>, Rebecca Caesar<sup>c</sup>, Jingwei Zhang<sup>a</sup>, Xun Li<sup>a</sup>, Van Trung Chu<sup>a</sup>, Anna Jauch<sup>d</sup>, Kristian Unger<sup>e,f</sup>, Daniel J. Hodson<sup>c</sup> , Altuna Akalin<sup>b</sup>, and Klaus Rajewsky<sup>a,1</sup>

<sup>a</sup>Department of Cancer Research, Max Delbrück Center for Molecular Medicine, 13215 Berlin, Germany; <sup>b</sup>Berlin Institute for Medical Systems Biology, Max Delbrück Center for Molecular Medicine, 10115 Berlin, Germany; <sup>c</sup>Wellcome–Medical Research Council Cambridge Stem Cell Institute, Department of Haematology, University of Cambridge, CB2 0AF Cambridge, United Kingdom; <sup>d</sup>Institute of Human Genetics, University Heidelberg, 69120 Heidelberg, Germany; <sup>e</sup>Research Unit of Radiation Cytogenetics, Helmholtz Zentrum München, 85764 Neuherberg, Germany; and <sup>f</sup>Department of Radiation Oncology, University Hospital, Ludwig Maximilian University Munich, 81377 Munich, Germany

Contributed by Klaus Rajewsky, April 22, 2020 (sent for review December 9, 2019; reviewed by Riccardo Dalla-Favera and Christian Muenz)

**Epstein-Barr virus (EBV) is a B cell transforming virus that causes B cell malignancies under conditions of immune suppression. EBV orchestrates B cell transformation through its latent membrane proteins (LMPs) and Epstein-Barr nuclear antigens (EBNAs). We here identify secondary mutations in mouse B cell lymphomas induced by LMP1, to predict and identify key functions of other EBV genes during transformation. We find aberrant activation of early B cell factor 1 (EBF1) to promote transformation of LMP1-expressing B cells by inhibiting their differentiation to plasma cells. EBV EBNA3A phenocopies EBF1 activities in LMP1-expressing B cells, promoting transformation while inhibiting differentiation. In cells expressing LMP1 together with LMP2A, EBNA3A only promotes lymphomagenesis when the EBNA2 target *Myc* is also overexpressed. Collectively, our data support a model where proproliferative activities of LMP1, LMP2A, and EBNA2 in combination with EBNA3A-mediated inhibition of terminal plasma cell differentiation critically control EBV-mediated B cell lymphomagenesis.**

Epstein-Barr virus | LMP1 | EBNA | B cell lymphomagenesis | plasma cell differentiation

**E**pstein-Barr virus (EBV) is a B lymphotropic  $\gamma$ -herpesvirus that is endemic in humans, with more than 90% of the population latently infected (1). EBV is the only known virus capable of in vitro transforming human B cells into continuously proliferating lymphoblastoid cell lines (LCLs). In healthy individuals proliferating EBV-infected B cells are eliminated by a T and NK cell-mediated immune response, restricting infection to rare memory B cells with no or limited viral gene expression (2). Immunocompromised patients fail to control infected B cells and are thus prone to develop EBV<sup>+</sup> B cell pathologies (2). A prominent example are EBV<sup>+</sup> posttransplant (PT) lymphoproliferative disorders (PTLDs) arising in up to 22% of patients undergoing immunosuppressive drug treatment after organ transplantation (3). EBV<sup>+</sup> PTLDs present as polymorphic or monomorphic disease, the latter mostly resembling activated B cell-like (ABC)-diffuse large B cell lymphoma (DLBCL) and less frequently, Hodgkin- (HL), or Burkitt-lymphoma (BL), or plasma cell (PC) neoplasms (3). PT-ABC-DLBCLs usually express the EBV growth program (called latency III) which also facilitates B cell-to-LCL transformation in vitro, suggesting that EBV is the main driving force in such tumors (1, 4). The EBV growth program involves expression of several noncoding RNAs, three latent membrane proteins (LMPs), and six Epstein-Barr nuclear antigens (EBNAs) (1). LMPs and EBNAs were shown to control key steps of B cell activation: LMP1 mimics an active CD40 receptor to mainly induce NF- $\kappa$ B and JNK signaling pathways (5, 6). LMP2A resembles a constitutively active B cell receptor (BCR), primarily activating PI3K and MAPK signaling (7–9). EBNA2 mimics NOTCH in binding to RBP-J and activating target genes, most notably *MYC* (10). EBNA3A and 3C

also bind RBP-J but serve as transcriptional repressors, epigenetically silencing the tumor suppressor genes *CDKN2A* (p16-INK4a/ARF) and *BCL2L1* (BIM) (11). Despite ample work on the activity of LMPs and EBNAs during in vitro transformation, their impact on B cell lymphomagenesis in vivo remains elusive. This is largely due to EBV not infecting small laboratory animals (12). Furthermore, modeling EBV pathologies in transgenic mice had limited success, with only LMP1-transgenic mice showing reliable B cell tumor development at old age (8, 13–18). More recently, EBV infection in mice reconstituted with human hematopoietic cells is successfully used to recapitulate virally driven B cell lymphomagenesis (19); yet this approach like the transformation of human B cells in vitro relies on infectious EBV, making it challenging to study the activity of single LMP or EBNA genes.

We previously developed a conditional transgenic mouse model that recapitulates EBV-driven lymphomagenesis in immunodeficient hosts (20). In this model, B cell-specific activation of a

## Significance

**Epstein-Barr virus (EBV) efficiently transforms human B cells and causes B cell lymphomagenesis especially in immunocompromised patients. We study this process in genetically engineered mice to untangle the interplay of EBV oncogenes. We find Epstein-Barr nuclear antigen (EBNA) 3A to have both oncogenic and tumor suppressive roles. First, EBNA3A promotes B cell transformation by inhibiting LMP-driven plasma cell differentiation, a function which can be mimicked by aberrant activation of early B cell factor 1 (EBF1). Second, EBNA3A blunts *Myc*-driven proliferation, rendering B cell transformation dependent on *Myc* activation by the EBV protein EBNA2. The presented mouse model thus highlights the role of EBV oncogenes in orchestrating B cell transformation through control of B cell differentiation and *Myc* levels.**

Author contributions: T.S., T.Y., T. Wirtz, T. Weber, X.L., and K.R. designed research; T.S., T.Y., and R.C. performed research; U.S., R.C., J.Z., V.T.C., A.J., K.U., D.J.H., and A.A. contributed new reagents/analytic tools; T.S., T.Y., J.R., A.J., and K.U. analyzed data; and T.S. and K.R. wrote the paper.

Reviewers: R.D.-F., Columbia University Medical Center; and C.M., University of Zürich. The authors declare no competing interest.

Published under the [PNAS license](https://www.pnas.org/licenses).

Data deposition: RNA sequencing, exome sequencing, and array comparative genomic hybridization (CGH) data are available at the GEO repository under accession no. [GSE136075](https://www.ncbi.nlm.nih.gov/geo/query/acc.cgi?acc=GSE136075).

<sup>1</sup>To whom correspondence may be addressed. Email: klaus.rajewsky@mdc-berlin.de or Thomas.Sommermann@mdc-berlin.de.

<sup>2</sup>T.Y. and J.R. contributed equally to this work.

This article contains supporting information online at <https://www.pnas.org/lookup/suppl/doi:10.1073/pnas.1921139117/-DCSupplemental>.

Rosa26 (R26) LMP1-transgene induces B cell proliferation followed by their T cell-mediated elimination. In T cell-deficient mice, LMP1-expressing B cells (LMP1 B cells) cause a lymphoproliferative disease (LPD) that within a few months spontaneously progresses to lymphoma. Strikingly, such LMP1-driven lymphomas (LMP1-Ls) are monoclonal, arguing that spontaneous somatic mutations are required to transform LMP1 B cells. We set out to identify such mutations in order to define pathways that must be engaged by EBV for successful B cell transformation. A recurrent activating mutation of the B cell transcription factor EBF1 turned out to be a functional proxy of the EBV gene EBNA3A in its interplay with other EBV oncogenes in B cell transformation.

## Results

### Ebf1 and Rel Are Aberrantly Activated in Mouse LMP1 Lymphomas.

Previously established LMP1-Ls were created on a mixed genetic background and without a reporter, rendering it challenging to prepare pure lymphoma samples for genetic analysis (20). We here combined a *R26LMP1-ires-huCD2<sup>stopf</sup>* allele (*R26LMP1<sup>stopf</sup>*) (21) with *Cd3ε<sup>KO</sup>* to confer T cell deficiency and *Cd19-Cre* for B cell-specific deletion of the floxed stop cassette (*stopf*) to allow LMP1 and huCD2-reporter expression on a C57BL/6 background. To create a lymphoma cohort, we transplanted fetal liver hematopoietic stem and progenitor cells (fHSPCs) from *Cd3ε<sup>KO</sup>;Cd19-Cre;R26LMP1<sup>stopf</sup>* mice into irradiated *Rag2<sup>KO/cγ</sup>* mice (tpLMP1 mice) (Fig. 1A). Within 7 mo, all tpLMP1 mice developed LMP1-Ls infiltrating liver, lung, and spleen (Fig. 1B and *SI Appendix, Fig. S1A*). In line with previous findings (20),

histologic analyses graded LMP1-Ls as CD10<sup>-</sup>, BCL6<sup>-</sup>, and MUM1<sup>+</sup> (*SI Appendix, Fig. S1A* and Table S1), resembling ABC-DLBCL (22). To separate LMP1-L cells from nontransformed LMP1 B cells (tpLMP1 B cells), we transplanted  $5 \times 10^6$  cells from tpLMP1 mice with primary tumors into secondary immunodeficient recipients. All secondary (2<sup>ry</sup>) LMP1-Ls were CD19<sup>+</sup> and expressed the LMP1 target FAS and a single immunoglobulin (Ig) isotype (*SI Appendix, Fig. S1B* and Table S1). Southern blot analysis for Ig-heavy chain rearrangements confirmed B cell origin and clonality of 2<sup>ry</sup>LMP1-Ls (*SI Appendix, Fig. S1C*). To define somatic driver mutations, we performed exome sequencing on 10 sorted 2<sup>ry</sup>LMP1-Ls. Tumors harbored between 16 and 60 clonal mutations (*SI Appendix, Fig. S1D* and Dataset S1). Mutations mostly altered noncoding regions. Mis- or nonsense mutations were rare and never involved the same protein coding sequence in independent tumors. As exome sequencing did not reveal obvious candidates for driver mutations, we performed array comparative genomic hybridization (CGH) to detect chromosomal aberrations. Besides expected copy number variations (CNV) in the Ig loci on Chr6 (*Igk*) and Chr12 (*Igh*), the most common CNVs were complete or partial gains of Chr11 and Chr15 (*SI Appendix, Fig. S1E* and Dataset S2). Interestingly, lymphomas 37 and 43 shared a copy number loss 3' of the IgH locus on Chr12 and a partial copy number gain of Chr11 (*SI Appendix, Fig. S1E* and *F*), a pattern indicative of a nonbalanced translocation between the respective loci (23). Indeed, multiplex fluorescence in situ hybridization (M-FISH) analysis of LMP1-L-derived cell lines (LMP1-CL) confirmed t(11;12) translocations in tumors 37 and 43 (Fig. 1C and *SI Appendix, Fig. S1G* and Table S2). Chimeric reads involving the

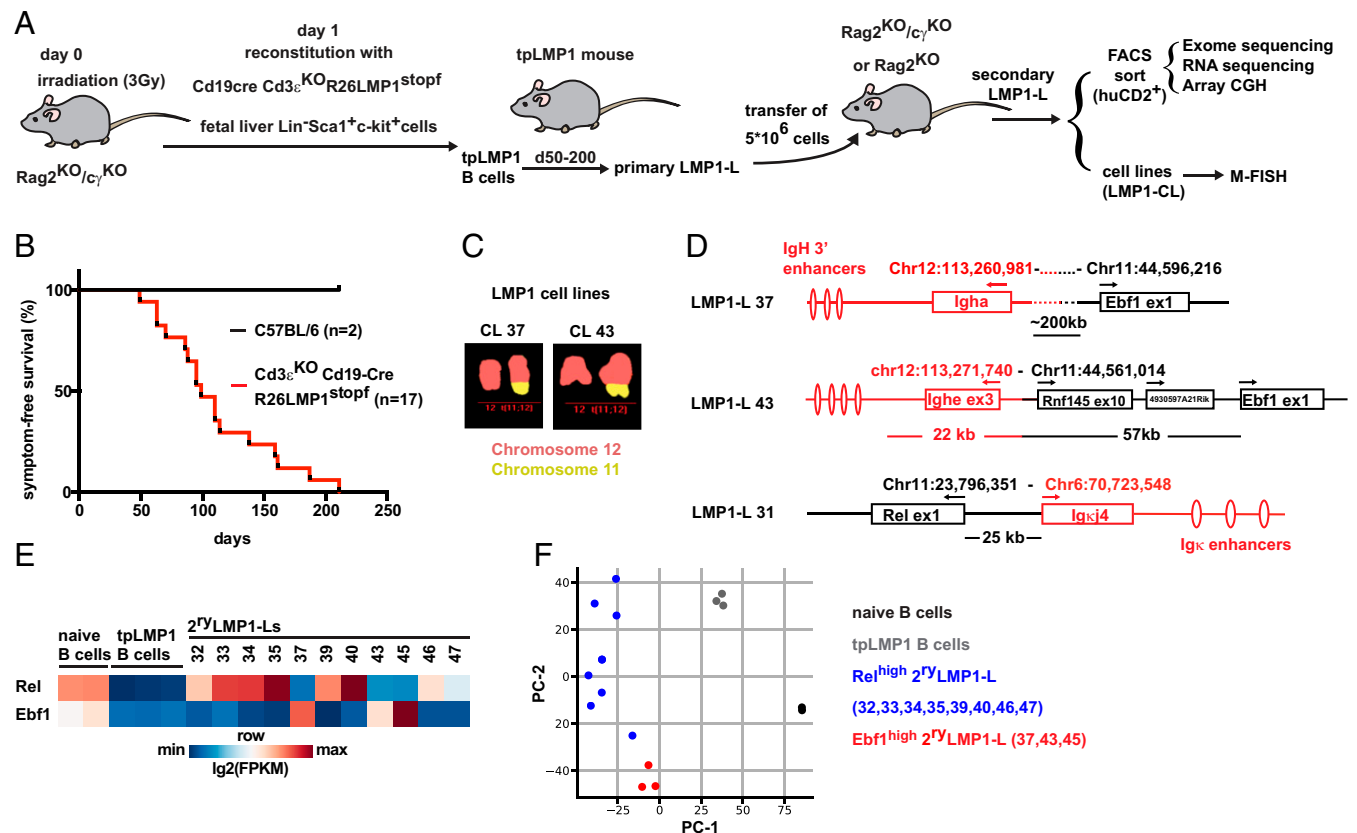


**Fig. 1. Ebf1 and Rel are aberrantly activated in LMP1 lymphomas.** (A) Experimental overview LMP1-L cohort. (B) Survival curve. (C) Representative M-FISH of t(11;12) translocations in LMP1-CLs 37 and 43. (D) Translocations in sorted (huCD2<sup>+</sup>) 2<sup>ry</sup>LMP1-Ls as determined by exome and Sanger sequencing (LMP1-L 31 and 43) or as suggested by CNVs in array CGH (LMP1-L 37). Arrows indicate ORF orientation (E and F) RNA sequencing of sorted splenic B cells (CD19<sup>+</sup>CD38<sup>+</sup>), tpLMP1 B cells (days 18 to 20 posttransplantation [p.t], huCD2<sup>+</sup>) and 2<sup>ry</sup>LMP1-Ls (huCD2<sup>+</sup>). (E) Heatmap showing fragments per kilobase of transcript per million mapped reads (FPKM)-normalized expression. (F) Principal component analysis on the 500 most-variable genes.

Ig loci in exome sequencing and subsequent Sanger sequencing of the chimeric locus in primary LMP1-Ls mapped the exact translocation in tumor 43 to *Ighe* exon 3 and intron 9 of *Rnfl45*, 57 kb upstream of the *Ebf1* gene (Fig. 1D, *SI Appendix*, Fig. S1 H and I, and *Dataset S3*). Exome sequencing reads did not span the translocation site in tumor 37, but revealed a translocation in 2<sup>Y</sup>LMP1-L 31 involving the *Igk* locus on Chr6 and Chr11 25 kb upstream of *Rel* (encoding NF- $\kappa$ B transcription factor c-Rel) (Fig. 1D, *SI Appendix*, Fig. S1 H and I, and *Dataset S3*). As translocation of genes into the proximity of Ig enhancers is a common mechanism to activate oncogenes in B cell tumors (24), we determined *Ebf1* and *Rel* expression by RNA sequencing of tpLMP1 B cells before and after transformation. Compared to naive B cells from C57BL/6 mice, nontransformed tpLMP1 B cells showed reduced expression of *Ebf1* and *Rel* (Fig. 1E). In contrast, all 2<sup>Y</sup>LMP1-Ls overexpressed one of the two genes, with *t*(11;12)-translocated tumors 37 and 43 expressing elevated *Ebf1* levels (Fig. 1E). Corresponding to the RNA-expression levels in the initial tumor, LMP1-CLs expressed elevated protein levels of EBF1 or c-Rel (*SI Appendix*, Fig. S1J). LMP1-CL 45 highly expressed c-Rel and EBF1, although the initial tumor was *Ebf1*<sup>high</sup>/*Rel*<sup>low</sup>. Taken together, *Ebf1* and *Rel* are recurrently activated in LMP1-Ls and were thus considered as secondary driver candidates. In nonsupervised principal component analysis on global RNA expression *Ebf1* and *Rel* expression formed separate tumor subgroups, further indicating that both genes define distinct LMP1-L subsets (Fig. 1F).

#### EBF1 or Rel Overexpression Supports Transformation of LMP1 B Cells.

To analyze the impact of LMP1/EBF1 or LMP1/c-Rel coexpression on naive B cells, we isolated CD43<sup>+</sup> B cells from *R26LMP1<sup>stopf</sup>* mice and induced LMP1-expression in vitro (iLMP1 B cells) by incubating the cells with HIV-TAT-coupled Cre-recombinase (TAT-Cre) (Fig. 2A). One day after TAT-Cre, iLMP1 B cells were transduced with retroviruses (RVs) encoding *GFP*, *Ebf1*, or *Rel*. Control-transduced iLMP1 B cells transiently expanded for 8 to 10 d (Fig. 2B). Strikingly, *Ebf1*- or *Rel*-transduced iLMP1 B cells continued to expand and turned into continuously proliferating mouse lymphoblastoid cell lines (EBF1-LCL, c-Rel-LCL) (Fig. 2B). *Ebf1* or *Rel* expression in anti-CD40 ( $\alpha$ CD40)/IL-4-stimulated control B cells did not promote proliferation. After 45 d, PCR analysis for diversity of VDJ rearrangements indicated oligoclonal outgrowth of EBF1-LCLs and c-Rel-LCLs (*SI Appendix*, Fig. S2A). Like human LCLs, these mouse LCLs aggregated in clumps and expressed the surface markers CD19, CD20, MHCII, Ig-light chain, ICAM, and FAS (*SI Appendix*, Fig. S2 B and C and *Table S3*) (25, 26). Also similar to human LCLs, CD23 was expressed only in a subset of mouse LCLs. CD3 $\epsilon$  (not expressed on LCLs) was expressed at low levels on one out of four analyzed EBF1-LCLs. EBF1-LCLs could be grown from ~2% of single-sorted *Ebf1*-transduced iLMP1 B cells, while c-Rel-LCLs rarely grew as single-cell clones (Fig. 2C). To validate their malignancy,  $3 \times 10^5$  freshly *Ebf1*- or *Rel*-transduced iLMP1 B cells were transferred into *Rag2<sup>KO</sup>c $\gamma$ <sup>KO</sup>* mice. Within 12 to 21 d all transplanted mice developed severe lymphoproliferative disease (Fig. 2D), with *Rel*- or *Ebf1*-expressing iLMP1 B cells expanding in liver and spleen (Fig. 2 E–G). Analysis for VDJ diversity did not indicate clonal selection in this timeframe (*SI Appendix*, Fig. S2D). Indeed, transfer of as few as  $1 \times 10^3$  *Ebf1*- or *Rel*-transduced iLMP1 B cells caused terminal lymphoproliferative disease within ~30 (LMP1/EBF1) or 60 d (LMP1/c-Rel) (Fig. 2D). Taken together, aberrant expression of *Ebf1* or *Rel* leads to an efficient transformation of mouse LMP1 B cells in vivo and in vitro. To determine whether combined LMP1/EBF1 or LMP1/c-Rel expression also supports expansion of human B cells, we made use of a recently published system to transduce primary human tonsillar germinal center B cells

(GCBs) (27). While single transduction of *Ebf1* or *Rel* had little impact on human GCBs, EBF1 and, to a minor extent c-Rel, indeed enhanced the expansion of LMP1-expressing GCBs (Fig. 2H).

**Rel Activation Induces LMP1/NF- $\kappa$ B Target Genes.** *Rel* overexpression in LMP1-Ls should elevate NF- $\kappa$ B target gene expression through increased nuclear c-Rel. Indeed, secondary *Rel*<sup>high</sup> LMP1-Ls and the *Rel/Igk* translocated lymphoma 31 expressed more (mostly nuclear) c-Rel than nontransformed tpLMP1 B cells and *Ebf1*<sup>high</sup> LMP1-Ls (*SI Appendix*, Fig. S3A). Furthermore, in our RNA-sequencing data, a set of previously described human LMP1/NF- $\kappa$ B target genes (26) was significantly more highly expressed in *Rel*<sup>high</sup> 2<sup>Y</sup>LMP1-Ls compared to *Ebf1*<sup>high</sup> 2<sup>Y</sup>LMP1-Ls and tpLMP1 B cells (*SI Appendix*, Fig. S3 B and C). Among these genes were the antiapoptotic Bcl2 family members *Bcl2l1* (Bcl-X), *Bcl2a1a*, and *Bcl2a1d* (A1a/d) (*SI Appendix*, Fig. S3D), which may well support B cell transformation.

**EBF1 Inhibits Plasma Cell Differentiation of LMP1 B Cells.** EBF1 is a transcription factor that is required to maintain B cell identity (28). During PC differentiation, *Ebf1* expression is silenced (29). As LMP1 suppressed *Ebf1* transcription (Fig. 1E), we wondered whether LMP1 induces B cell differentiation toward PCs. Indeed, compared to naive splenic B cells, tpLMP1 B cells showed low expression of the B cell transcription factor genes *Pax5*, *Ets1*, *Bcl6*, and *Bach2* and elevated transcription of the master PC transcription factor gene *Prdm1* (Fig. 3A). Furthermore, tpLMP1 B cells expressed the PC-surface marker CD138 (Fig. 3 B and D). In contrast, *Ebf1*<sup>high</sup> LMP1-Ls showed neither CD138 surface staining nor elevated levels of *Prdm1* mRNA (Fig. 3 A, C, and D). To test whether *Ebf1* induction is sufficient to block LMP1-mediated PC differentiation in vitro, we performed RNA sequencing on retrovirally transduced iLMP1 B cells. *Ebf1* overexpression blunted *Prdm1* induction and shifted the global mRNA expression pattern of iLMP1 B cells from PC- to GCB-like (Fig. 3 E and F). *Ebf1* overexpression also blunted plasma blast (PB) differentiation of naive B cells cultured on CD40-L and BAFF-expressing feeders (40LB) (30) (*SI Appendix*, Fig. S3 E and F). Despite recent reports that c-Rel can suppress PC differentiation (31), *Rel* overexpression had little impact on *Prdm1* expression in iLMP1 B cells and did not inhibit PB differentiation of cytokine-stimulated wild-type B cells (Fig. 3E and *SI Appendix*, Fig. S3 E and F). Furthermore, *Ebf1* but not *Rel* overexpression blunted PB differentiation of iLMP1 B cells when transplanted into *Rag2<sup>KO</sup>c $\gamma$ <sup>KO</sup>* mice (*SI Appendix*, Fig. S3G). GFP control transduced cells did not survive long enough after transplantation to be analyzed. Although c-Rel alone did not impact PB differentiation, the majority of *Rel*<sup>high</sup> LMP1-Ls showed low or no CD138 expression (Fig. 3D), arguing that *Rel*<sup>high</sup> LMP1-Ls also benefit from a loss of PC differentiation. Taken together, loss of PC differentiation is a general feature of LMP1-driven lymphomagenesis, caused either by EBF1 activation or unknown events in the *Rel*<sup>high</sup> cases. Importantly, suppression of PC differentiation is considered to be a key event in NF- $\kappa$ B-driven ABC-DLBCL development (32), suggesting that EBF1-suppressive effects on LMP1-induced PC differentiation are critical for the transformation of LMP1 B cells to DLBCL-like tumors.

**EBNA3A Inhibits PC Differentiation in Transgenic Mice.** We next set out to define EBV growth program genes whose role in transformation and differentiation might be mimicked by aberrant EBF1-activation. As LMP2A, unlike EBF1, was reported to promote PC differentiation (33) we focused on EBNA genes. To determine their impact on LMP1-driven transformation, we retrovirally overexpressed individual HA-tagged EBNA genes in iLMP1 B cells. EBNA2 expression was below the detection limit

and could therefore not be studied (*SI Appendix, Fig. S4A*). All other EBNA3s were readily detectable in the nucleus of transduced iLMP1 B cells, but only EBNA3A supported cell expansion (Fig. 4A and *SI Appendix, Fig. S4A*). To study EBNA3A in vivo, we generated a *R26CAG-EBNA3A-HA-ires-BFP<sup>stopf</sup>* allele (*R26EBNA3A<sup>stopf</sup>*) and a *R26CAG-BFP-ires-huCD2<sup>stopf</sup>* reporter allele (*R26BFP<sup>stopf</sup>*) (*SI Appendix, Fig. S4 B and C*). Both novel *R26* alleles were combined with *Cd19-Cre<sup>cre/+</sup>* (*Cd19-Cre*) for B cell-specific transgene expression. *Cd19-Cre;R26EBNA3A<sup>stopf</sup>* and *Cd19-Cre;R26BFP<sup>stopf</sup>* mice expressed the BFP reporter in the

majority of (*CD19<sup>+</sup>B220<sup>+</sup>*) splenic B cells (Fig. 4B). HA-coimmunoprecipitation experiments in  $\alpha$ CD40/IL-4-stimulated splenic B cells confirmed EBNA3A-protein expression in *Cd19-Cre;R26EBNA3A<sup>stopf</sup>* B cells and conserved EBNA3A binding to its core interaction partner RBP-J (*SI Appendix, Fig. S4D*). *Cd19-Cre;R26EBNA3A<sup>stopf</sup>* and *Cd19-Cre;R26BFP<sup>stopf</sup>* mice had a normal life expectancy (Fig. 4C). Furthermore, EBNA3A expression in B cells did not impact splenic size, cellularity, and absolute B cell numbers (*SI Appendix, Fig. S4E*). *Cd19-Cre;R26EBNA3A<sup>stopf</sup>* mice had a normal frequency of BFP<sup>+</sup> pro, pre, and immature B cells in

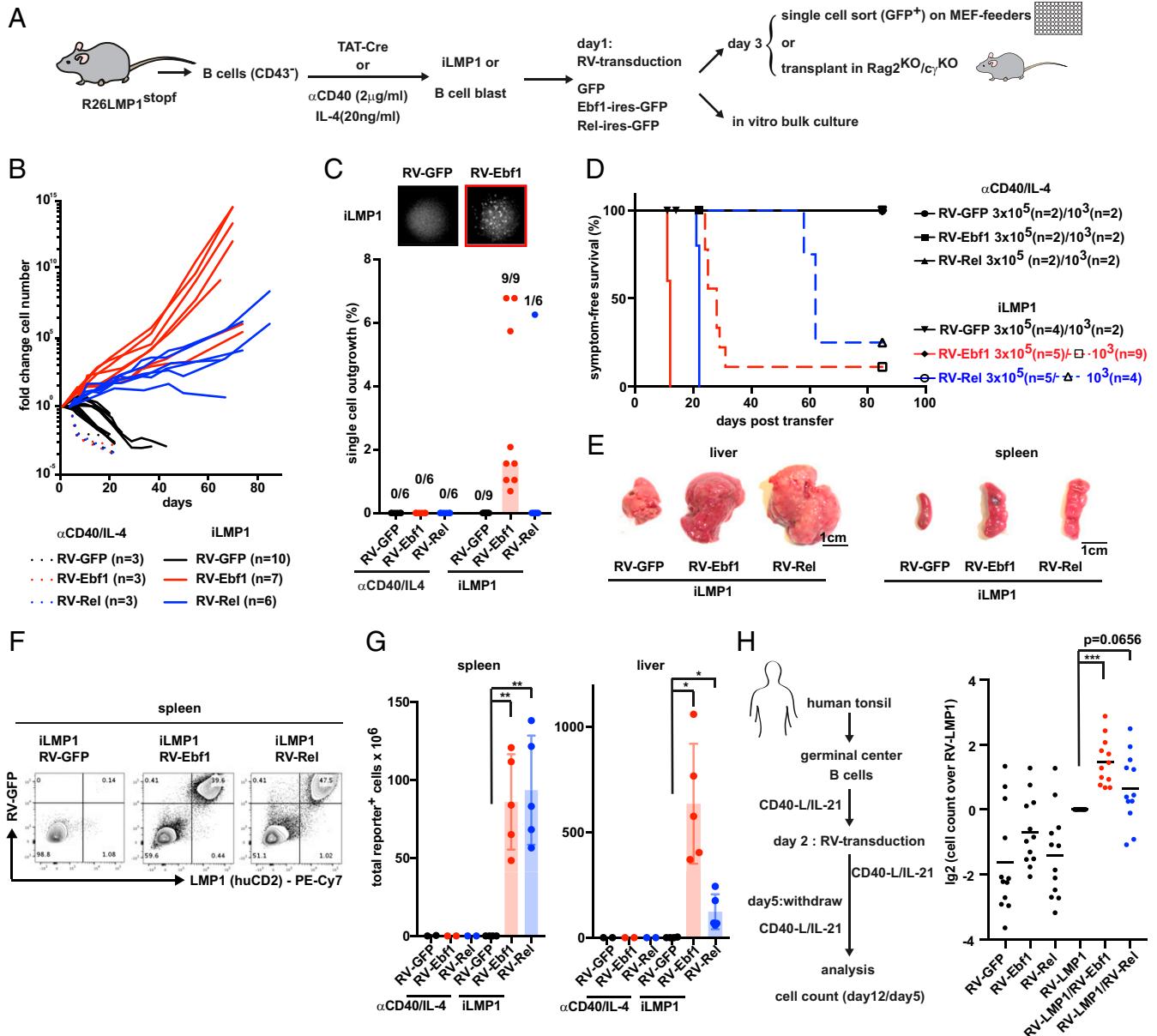


**Fig. 2. *Ebf1* or *Rel* overexpression supports transformation of LMP1 B cells.** (A) Experimental overview of A–G. (B) Growth curve of transduced (*GFP<sup>+</sup>*) cells. (C) Quantification of outgrowing single-sorted transduced (*GFP<sup>+</sup>*) cells on mouse embryonic fibroblast (MEF) feeder. Bars represent median outgrowth frequency. Number of biological replicates showing any outgrowth is indicated. Images show representative wells on day 21 post TAT-cre. (D) Survival curve of transplanted *Rag2<sup>KO</sup>c<sub>y</sub><sup>KO</sup>* mice. (E–G) Analysis of *Rag2<sup>KO</sup>c<sub>y</sub><sup>KO</sup>* mice transplanted with  $3 \times 10^5$  *GFP<sup>+</sup>* cells. Analysis was performed at symptom onset or between days 11 and 22 (control groups). (E) Representative organ images day 11 (RV-GFP/RV-*Ebf1*) and day 21 (RV-*Rel*). (F) Fluorescence-activated cell sorting (FACS) analysis of splenocytes from E. (G) Cell count of *GFP<sup>+</sup>/huCD2<sup>+</sup>* cells in indicated organs.  $n = 2$  ( $\alpha$ CD40/IL-4 treated groups);  $n = 4$  (iLMP1 RV-GFP);  $n = 5$  (iLMP1 RV-*Ebf1* or iLMP1 RV-*Rel*). (H) Human tonsillar GCBs were cultured on CD40-L/IL-21 feeder cells and transduced with RVs encoding GFP, LMP1-ires-GFP, *Ebf1*-ires-mCherry, or *Rel*-ires-mCherry. Starting day 5, cells were cultured on feeders without CD40-L/IL-21. Fold change of reporter<sup>+</sup> cell number on day 12 over day 5 is presented;  $n = 12$ . All data are presented as mean  $\pm$  SD. Significance was calculated by Welch's *t* test (G) or one-sample *t* test (H). (\* $P < 0.05$ ; \*\* $P < 0.005$ ; \*\*\* $P < 0.0005$ ).

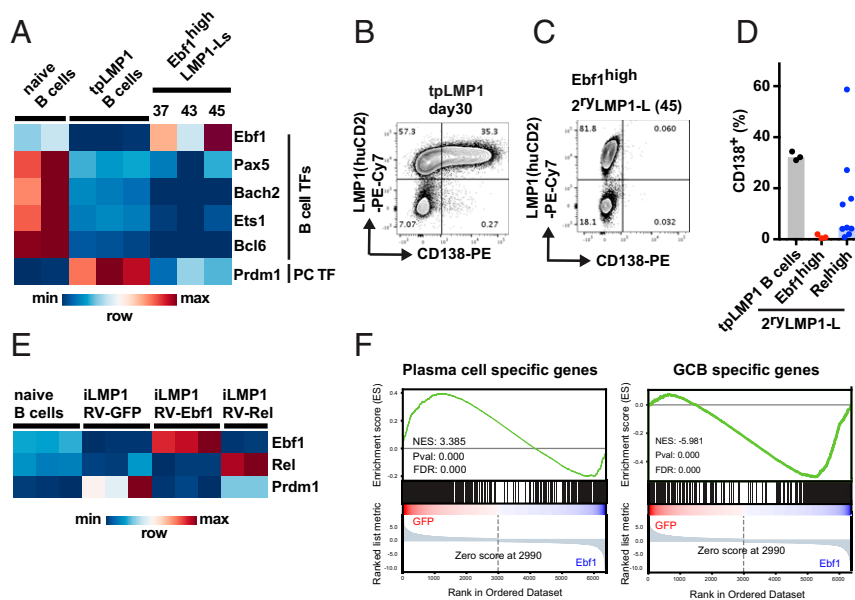


**Fig. 3.** Ebf1 inhibits PC differentiation of LMP1 B cells. (A–D) Further analysis of  $2^7$ LMP1-Ls from Fig. 1. (A) Heatmap showing FPKM-normalized expression of B cell and PC transcription factors (TFs) in RNA sequencing. (B) FACS analysis of splenocytes from tpLMP1 mice before lymphomagenesis (day 30 post-transplant). (C) FACS analysis of a representative splenic *Ebf1*<sup>high</sup>  $2^7$ LMP1-L. (D) Quantification of CD138 expression on huCD2<sup>+</sup> cells in B and C. Bars indicate median.  $n = 3$  (tpLMP1 and *Ebf1*<sup>high</sup> LMP1-L),  $n = 9$  (*Rel*<sup>high</sup> LMP1-L). (E and F) RNA sequencing of iLMP1 B cells transduced on day 1 with RVs encoding GFP, *Ebf1*-ires-GFP, or *Rel*-ires-GFP. RNA was isolated from FACS-sorted (GFP<sup>+</sup>/huCD2<sup>+</sup>) cells on day 6 post TAT-Cre. Naive splenic B cells (CD19<sup>+</sup>/CD38<sup>+</sup>) from wild-type mice are presented as a control. (E) Heatmap showing FPKM-normalized expression. (F) Gene set enrichment analysis of a gene set differentially expressed in splenic PCs over GCBs (29) run in the space of genes differentially expressed between GFP- and *Ebf1*-transduced iLMP1 B cells on day 6.

the bone marrow, while the frequency of reporter<sup>+</sup> mature B cells in the spleen was mildly reduced (Fig. 4D), an effect at least partially attributable to limited separation of BFP<sup>+</sup> and BFP<sup>-</sup> B cells. Although their number was almost normal, EBNA3A<sup>+</sup> splenic B cells showed a disturbed marginal zone B cell (MZB) and follicular B cell (FOB) surface staining, with CD23<sup>low</sup>CD21<sup>+</sup> MZBs being absent and numbers of CD23<sup>+</sup>CD21<sup>low</sup> FOBs being reduced (SI Appendix, Fig. S4F). Instead, most EBNA3A<sup>+</sup> B cells were CD23<sup>low</sup>CD21<sup>low</sup>. Despite these alterations, all EBNA3A<sup>+</sup> cells expressed surface IgM and IgD levels similar to control FOBs (SI Appendix, Fig. S4F). Also, spleens of *Cd19-Cre;R26EBNA3A*<sup>stopf</sup> mice had a normal follicular structure, including EBNA3A<sup>+</sup> B cells locating to B cell follicles and the marginal zone (SI Appendix, Fig. S4G). Although EBNA3A was expressed in more than 80% of mature splenic B cells, CD138<sup>+</sup>CD267 (TAC1)<sup>+</sup> PCs of *Cd19-Cre;R26EBNA3A*<sup>stopf</sup> mice rarely expressed EBNA3A (Fig. 4E). Furthermore, the frequency of antibody-secreting cells (ASCs) among BFP<sup>+</sup> cells in the bone marrow of *Cd19-Cre;R26EBNA3A*<sup>stopf</sup> mice was more than sevenfold reduced compared to *Cd19-Cre;R26BFP*<sup>stopf</sup> mice (Fig. 4F). To address whether EBNA3A<sup>+</sup> B cells can differentiate in vitro, we cultured BFP<sup>+</sup> FOBs from *Cd19-Cre;R26EBNA3A*<sup>stopf</sup> and *Cd19-Cre;R26BFP*<sup>stopf</sup> mice on 40LB feeders. While FOBs from control mice readily differentiated into CD138<sup>+</sup> plasma blasts, the majority of EBNA3A<sup>+</sup> FOBs remained CD138<sup>-</sup> (SI Appendix, Fig. S4H). Importantly,  $\alpha$ CD40/IL-4-stimulated FOBs from *Cd19-Cre;EBNA3A*<sup>stopf</sup> mice expanded better than control cells, arguing that CD40 signaling in EBNA3A<sup>+</sup> B cells is rather elevated than impaired (SI Appendix, Fig. S4I). Similarly, lipopolysaccharide (LPS) and IL-4 stimulation did not induce PC differentiation of EBNA3A<sup>+</sup> FOBs (SI Appendix, Fig. S4J). Taken together, EBNA3A expression in mouse B cells does not promote lymphomagenesis, has little impact on early B cell development, distorts differentiation of mature B cell subsets (at least at surface marker level), and strongly inhibits terminal PC differentiation.

**EBNA3A Inhibits PC Differentiation and Supports Expansion of LMP1 B Cells.** To evaluate the impact of EBNA3A on proliferation and differentiation of LMP1 B cells, we isolated B cells from *R26LMP1*<sup>stopf</sup>; *R26EBNA3A*<sup>stopf</sup> mice and activated transgene expression by TAT-Cre treatment (iLMP1/EBNA3A B cells). iLMP1/EBNA3A B cells expanded more than iLMP1 B cells, with EBNA3A supporting cell proliferation and inhibiting apoptosis (Fig. 5 A–C). RNA sequencing on day 6 revealed attenuated *Prdm1* expression in iLMP1/EBNA3A B cells (Fig. 5D). This effect was independent of *Ebf1*, as EBNA3A did not restore *Ebf1* expression in these cells. In human B cells, *CDKN2A* and *BCL2L1* are considered as EBNA3As key target genes (11). In iLMP1/EBNA3A B cells, EBNA3A severely blunted LMP1-induced *Cdkn2a* expression, while the impact on *Bcl2l1* levels was more modest (SI Appendix, Fig. S5 A and B). Yet, deleting *Cdkn2a* or *Bcl2l1* ORFs by retroviral delivery of sgRNAs into iLMP1/CAS9 B cells did not promote cell expansion (SI Appendix, Fig. S5 C and D), arguing that EBNA3A function extends beyond the suppression of *Cdkn2a* or *Bcl2l1*.

To test the impact of combined EBNA3A and LMP1 expression on B cells in vivo, we transplanted *Cd3 $\epsilon$* <sup>KO</sup>; *Cd19-Cre;R26LMP1*<sup>stopf</sup>; *R26EBNA3A*<sup>stopf</sup> fHSPCs into irradiated *Rag2*<sup>KO</sup> *c $\gamma$* <sup>KO</sup> mice (tpLMP1/EBNA3A). In contrast to tpLMP1 mice, tpLMP1/EBNA3A mice developed terminal LPD within 40 d after reconstitution (Fig. 5E). Spleens of tpLMP1/EBNA3A mice were dramatically enlarged and filled with LMP1<sup>+</sup>/EBNA3A<sup>+</sup> B cells (Figs. 5 F and G and SI Appendix, Fig. S5E). Analysis of VDJ rearrangements in splenocytes of tpLMP1/EBNA3A mice did not indicate clonal B cell expansion at termination (SI Appendix, Fig. S5F). Compared to tpLMP1 B cells tpLMP1/EBNA3A B cells showed reduced CD138 expression and antibody secretion (Figs. 5 G and H and SI Appendix, Fig. S5E). Thus, EBNA3A, like EBF1, facilitates polyclonal expansion of LMP1 B cells while inhibiting their differentiation to PBs,

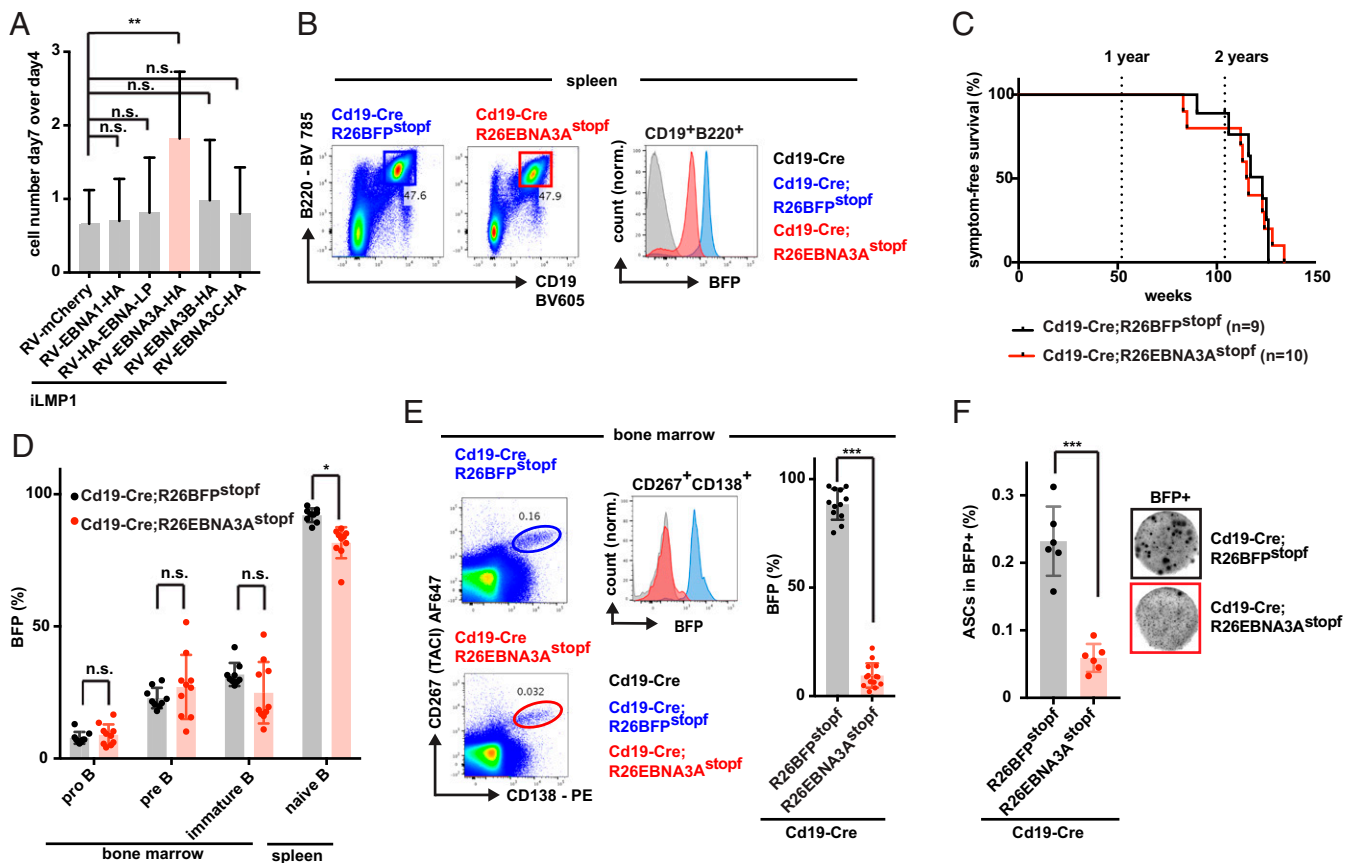


**Fig. 4.** EBNA3A inhibits PC differentiation. (A) iLMP1 B cells were transduced with RVs encoding mCherry or indicated EBNA3s (reported by ires-mCherry). FACS-based quantification of mCherry<sup>+</sup> cells day 7 over day 4 is presented ( $n = 5$ ). (B–F) Analysis of *Cd19-cre;R26EBNA3A<sup>stopf</sup>* and *Cd19-cre;R26BFP<sup>stopf</sup>* mice. (B) Representative FACS analysis of spleens. (C) Survival curve. (D) Quantification of BFP expression in bone marrow pro (CD93<sup>+</sup>B220<sup>+</sup>IgM<sup>-</sup>IgD<sup>-</sup>CD19<sup>+</sup>c-kit<sup>low</sup>), pre (CD93<sup>+</sup>B220<sup>+</sup>IgM<sup>+</sup>IgD<sup>-</sup>), and splenic mature (CD93<sup>-</sup>B220<sup>+</sup>IgM<sup>+</sup>IgD<sup>+</sup>) B cells.  $n = 9$  (*Cd19-Cre;BFP<sup>stopf</sup>*)  $n = 10$  (*Cd19-Cre;EBNA3A<sup>stopf</sup>*). (E) Representative FACS analysis and quantification of BFP expression in bone marrow (CD138<sup>+</sup>CD267<sup>+</sup>) PCs;  $n = 12$  (*Cd19-Cre;BFP<sup>stopf</sup>*)  $n = 14$  (*Cd19-Cre;EBNA3A<sup>stopf</sup>*). (F) Elispot for total ASCs in sorted BFP<sup>+</sup> bone marrow cells;  $n = 6$ . Images show representative wells with  $4 \times 10^4$  cells. All data are presented as mean  $\pm$  SD. Significance was calculated using a one-way ANOVA with  $P$  value adjusted via Dunnett (A), two-way ANOVA with Sidak's multiple comparisons test (D), Mann–Whitney  $U$  test (E), and Welch's  $t$  test (F). (\* $P < 0.05$ ; \*\* $P < 0.005$ ; \*\*\* $P < 0.0005$ ; n.s., nonsignificant).

suggesting that EBNA3A substitutes for EBF1 during EBV-driven PTLD development.

**EBF1 and REL Expression in Human PT-DLBCLs.** Given the impact of c-Rel and EBF1 on LMP1-driven B cells in the mouse model, we wondered whether LMP1 expression in human PT-DLBCLs positively correlates with *REL* activation, while *EBF1* might be specifically up-regulated in LMP1<sup>+</sup>/EBNA3A<sup>-</sup> cases. Alternatively, the presence of the full EBV genome in the human disease might alleviate the need for *REL* or *EBF1* activation. We therefore correlated expression of *EBF1* and *REL* with EBV-infection and -latency status in a published human PT-ABC-DLBCL dataset (34). PT-DLBCL datasets comparing exome mutations and amplifications were either too small to be informative (35) or did not report EBV latency II cases (36–38). Datasets reporting unbiased translocations in PT-DLBCLs were not available. In the expression analysis, latency II PT-ABC-DLBCLs (LMP1/2a;EBNA1) expressed rather less *EBF1* than latency III cases (LMP1/2a;EBNA1/LP/2/3A-C) (SI Appendix, Fig. S5G), arguing that the absence of EBNA3A in latency II tumors does not commonly entail EBF1 activation. Furthermore, *REL* levels, in line with other reports (39, 40), appeared independent of EBV infection. Together these data suggest that the presence of the

EBV genome alleviates the need for *REL* or *EBF1* activation in human PT-ABC-DLBCLs.

**EBNA3A Inhibits PC Differentiation of LMP1- and LMP2A-Expressing B Cells.** In the EBV growth program, LMP1 and EBNA3A are coexpressed with LMP2A, which by itself promotes proliferation and PC differentiation of LMP1-expressing mouse GCBs (41, 42). To evaluate whether lymphomagenesis of GCB cells expressing both LMPs also requires disruption of PC differentiation, we transferred  $3 \times 10^6$  B cells from *Cy1-Cre* (GCB specific) *R26LMP1<sup>stopf</sup>;R26LMP2A<sup>stopf</sup>* mice into *Rag2<sup>KO</sup>* mice (Fig. 6A). Transferred cells contained merely 100 to 300 LMP1<sup>+</sup>/2A<sup>+</sup> GCBs as these cells are continuously eliminated by T cells (Fig. 6B). In the reconstituted mice, LMP1<sup>+</sup>/2A<sup>+</sup> GCBs proliferated strongly and overwhelmingly differentiated into CD138<sup>+</sup>CD19<sup>low</sup> PCs within 17 to 28 d (Fig. 6B and SI Appendix, Fig. S6A). When aged, the reconstituted mice developed CD19<sup>+</sup>CD138<sup>-</sup>LMP1<sup>+</sup>/2A<sup>+</sup> B cell lymphomas (Fig. 6 C–E). One mouse developed a CD19<sup>+</sup>CD138<sup>-</sup>LMP1<sup>+</sup>/2A<sup>-</sup> B cell lymphoma (SI Appendix, Fig. S6B). Thus, upon transfer into an immunodeficient environment, LMP1<sup>+</sup>/2A<sup>+</sup> GCBs proliferate and rapidly differentiate to PCs. Yet, transformation is restricted to LMP1<sup>+</sup>/2A<sup>+</sup> GCBs that do not undergo PC differentiation.

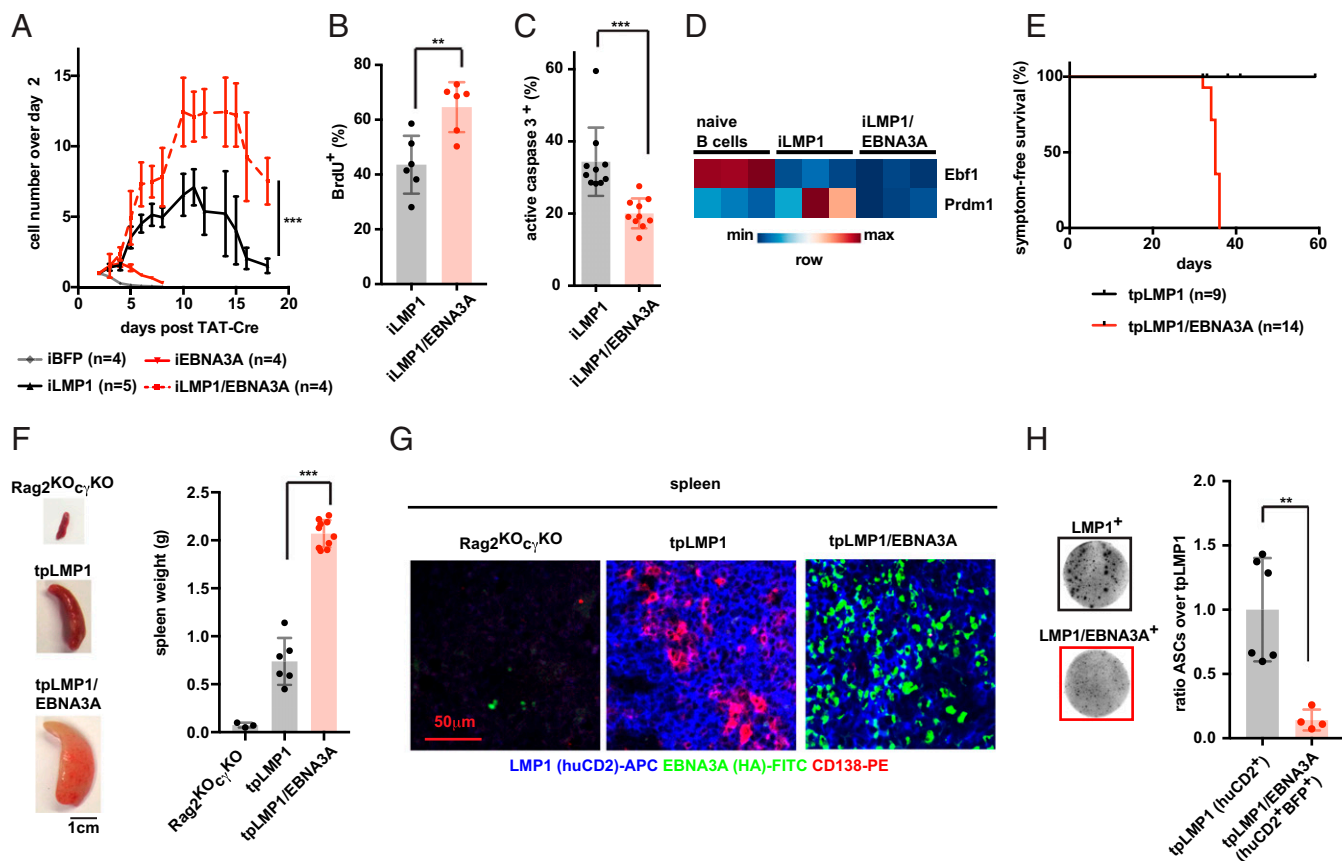


**Fig. 5.** EBNA3A inhibits PC differentiation and supports expansion of LMP1 B cells. (A–D) iBFP, iEBNA3A, iLMP1, and iLMP1/EBNA3A B cells. (A) Growth curve of bulk cultured cells.  $n = 4$ ,  $n = 5$  (iLMP1). (B) FACS-based quantification of BrdU uptake on day 6 post TAT-Cre.  $n = 6$ . (C) FACS-based quantification of active-caspase 3 on day 6 post TAT-Cre.  $n = 10$ . (D) Heatmap showing FPKM-normalized gene expression in RNA sequencing performed on sorted hucd2<sup>+</sup> (iLMP1) or hucd2<sup>+</sup>BFP<sup>+</sup> (iLMP1/EBNA3A) cells day 6 post TAT-Cre. Splenic naive (CD19<sup>+</sup>CD38<sup>+</sup>) B cells (from Fig. 3E) serve as a control. (E–H) Rag2<sup>KO</sup>cy<sup>KO</sup> mice were reconstituted with fHSPCs from *Cd3e*<sup>KO</sup>; *Cd19-Cre*; *R26LMP1*<sup>stopf</sup> (tpLMP1) or *Cd3e*<sup>KO</sup>; *Cd19-Cre*; *R26LMP1*<sup>stopf</sup>/*EBNA3A*<sup>stopf</sup> (tpLMP1/EBNA3A) mice. (E) Survival curve. (F) Representative image of spleens and quantification of splenic weight at symptom onset (tpLMP1/EBNA3A) or days 32 to 41 p.t. (tpLMP1);  $n = 3$  (Rag2<sup>KO</sup>cy<sup>KO</sup>),  $n = 6$  (tpLMP1),  $n = 10$  (tpLMP1/EBNA3A). (G) Immunohistology on splenic sections day 36 p.t. (representative of three independent mice per group). Splenic section of a Rag2<sup>KO</sup>cy<sup>KO</sup> mouse is presented as negative control. (H) ELISPOT for total ASCs in sorted reporter<sup>+</sup> splenic cells at symptom onset or days 32 to 41 p.t. (tpLMP1). Quantification was normalized to mean ASC frequency in tpLMP1 conditions. Images show representative wells with  $1.5 \times 10^5$  cells.  $n = 6$  (tpLMP1),  $n = 4$  (tpLMP1/EBNA3A). All data are presented as mean  $\pm$  SD. Significance was calculated using a Student's *t* test (A–C and F) or Welch's *t* test (H). (\*\* $P < 0.005$ ; \*\*\* $P < 0.0005$ ).

To allow in vivo coexpression of EBNA3A with both LMPs we generated an *R26LMP1t2aLMP2A*<sup>stopf</sup> allele that upon deletion of the stop cassette expresses both LMPs through a 2A-self cleavage peptide (SI Appendix, Fig. S6C). Compared to the expression from separate R26 alleles, LMP1 expression in TAT-Cre-treated *R26LMP1t2aLMP2A*<sup>stopf</sup> B cells (iLMP1\_2A B cells) was about twofold reduced, while LMP2A expression was comparable (SI Appendix, Fig. S6D). Still, the LMP1 target FAS was induced to similar levels in iLMP1/2A and iLMP1\_2A B cells, indicating robust NF- $\kappa$ B activation under both conditions (SI Appendix, Fig. S6E). iLMP1\_2A B cells proliferated extensively, expressed more *Prdm1* than iLMP1 B cells, and differentiated to antibody-secreting CD138<sup>+</sup>/B220<sup>low</sup> PCs within 9 d of culture (Fig. 6F and SI Appendix, Fig. S6F and G). iLMP2A cells expanded little and did not differentiate to PCs in their lifespan (SI Appendix, Fig. S6H and I). In contrast to iLMP1\_2A B cells, iLMP1\_2A/EBNA3A B cells showed blunted *Prdm1* expression, CD138 surface staining, and antibody secretion (Fig. 6F and G and SI Appendix, Fig. S6F). Overexpression of *Prdm1* in iLMP1\_2A/EBNA3A B cells allowed their differentiation to antibody-secreting CD138<sup>+</sup>/B220<sup>low</sup> PCs (SI Appendix, Fig. S6J and K). Notably, the inhibition of PC differentiation was specific

to EBNA3A as retroviral transduction of EBNA1, -LP, -3B, and -3C failed to inhibit differentiation of iLMP1\_2A B cells (SI Appendix, Fig. S6L). Taken together, combined expression of LMP1 and LMP2A from a single allele drives proliferation and rapid PC differentiation of B cells, which is inhibited by EBNA3A via *Prdm1* suppression.

**Transformation of LMP1- and LMP2A-Expressing B Cells Requires Overexpression of EBNA3A and Myc.** To test the impact of combined expression of LMP1, LMP2A, and EBNA3A on B cells in vivo, we reconstituted Rag2<sup>KO</sup>cy<sup>KO</sup> mice with fHSPCs from *Cd3e*<sup>KO</sup>; *Cd19-Cre*; *R26LMP1t2aLMP2A*<sup>stopf</sup> (tpLMP1\_2A mice) or *Cd3e*<sup>KO</sup>; *Cd19-Cre*; *R26LMP1t2aLMP2A*<sup>stopf</sup>; *R26EBNA3A*<sup>stopf</sup> (tpLMP1\_2A/EBNA3A mice). tpLMP1\_2A mice developed terminal LPD symptoms within 30 to 60 d (Fig. 6H), with LMP1\_2A expressing PCs accumulating in the spleen (SI Appendix, Fig. S6M and N). Surprisingly, tpLMP1\_2A/EBNA3A mice did not show an accelerated disease progression (Fig. 6H) and developed a slightly less severe splenomegaly (SI Appendix, Fig. S6O), suggesting that EBNA3A does not promote expansion of LMP1\_2A B cells. Indeed, a majority of splenocytes in tpLMP1\_2A/EBNA3A mice had escaped Cre-mediated

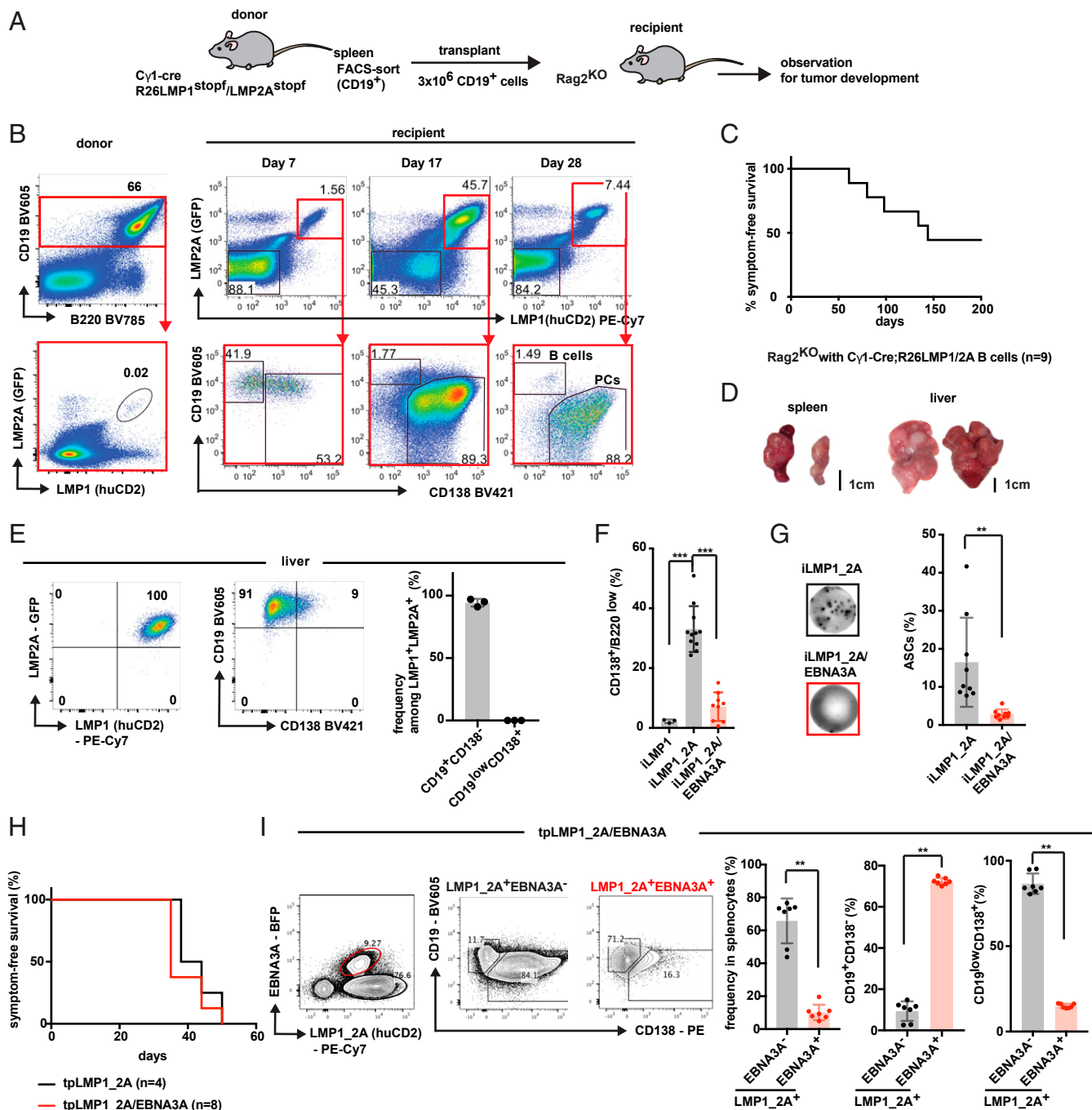


**Fig. 6. EBNA3A blocks PC differentiation of LMP1 and LMP2A B cells.** (A) Experimental overview of B–E. (B) Representative FACS analysis of spleens from donor animals and recipient animals at days 7 to 28 p.t. (quantification in *SI Appendix*, Fig. S6A). (C) Survival curve. (D) Representative images of LMP1/2A<sup>+</sup> lymphomas arising in C. (E) Representative FACS analysis and quantification of CD19/CD138 expression on huCD2<sup>+</sup>GFP<sup>+</sup> cells in lymphomas arising in C; *n* = 3. (F and G) iLMP1, iLMP1\_2A, and iLMP1\_2A/EBNA3A B cells analyzed on day 9 post TAT-Cre. (F) FACS-based quantification of CD138<sup>+</sup>/B220<sup>low</sup> PCs; *n* = 3 (iLMP1), *n* = 11 (iLMP1\_2A), *n* = 9 (iLMP1\_2A/EBNA3A). (G) Elispot for total ASCs among sorted reporter<sup>+</sup> cells. Images show representative wells with 120 cells; *n* = 9. (H and I) Rag2<sup>KO</sup>Cγ1<sup>KO</sup> mice were reconstituted with fHSPCs from *Cd3ε<sup>KO</sup>;Cd19-Cre R26LMP1\_LMP2A<sup>stopf</sup>* (tpLMP1\_2A) or *Cd3ε<sup>KO</sup>;Cd19-Cre R26LMP1\_LMP2A<sup>stopf</sup>;EBNA3A<sup>stopf</sup>* (tpLMP1\_2A/EBNA3A) mice. (H) Survival curve. (I) Representative FACS analysis of splenocytes from tpLMP1\_2A/EBNA3A mice at symptom onset. Quantifications shows expression of LMP1\_2A (huCD2<sup>+</sup>) and EBNA3A (BFP<sup>+</sup>) in whole splenocytes or CD19/CD138 expression on indicated populations. *n* = 7. All data are presented as mean ± SD. Significance was calculated using a Mann–Whitney *U* test (G and I), or one-way ANOVA with *P* value adjusted via Dunnett (F). (\*\**P* < 0.005; \*\*\**P* < 0.0005).

recombination of the EBNA3A allele and expressed only LMP1\_2A (Fig. 6I). This was despite EBNA3A still suppressing LMP1\_2A-driven PC differentiation in the fraction of B cells that had recombined both alleles (Fig. 6I). To determine why

EBNA3A expression is counterselected in LMP1\_2A B cells, we compared proliferation and survival of iLMP1\_2A and iLMP1\_2A/EBNA3A B cells in vitro. Both cell types expanded at similar rates (*SI Appendix*, Fig. S6P). EBNA3A inhibited caspase



3 activation (*SI Appendix, Fig. S6Q*) but, in stark contrast to its activity in LMP1-expressing B cells, blunted BrdU uptake (Fig. 7A). This suggests that EBNA3A has opposing effects on proliferation and cell survival in B cells expressing both LMPs. In vitro, inhibition of apoptosis and proliferation appear to counterbalance each other, allowing similar expansion dynamics. In vivo, the reduced proliferation might outweigh antiapoptotic effects and cause counterselection of EBNA3A-expressing cells. EBNA3A overexpression was previously reported to suppress proliferation of human LCLs by inhibiting *MYC* transcription (43). Similarly, we find iLMP1\_2A/EBNA3A B cells to express less *Myc* mRNA and protein compared to iLMP1\_2A B cells

(Fig. 7B and C). In LMP1 B cells, EBNA3A did not suppress *Myc* (Fig. 7B and *SI Appendix, Fig. S5B*). Retroviral overexpression of *Myc* promoted BrdU uptake and cell cycle and cell expansion of iLMP1\_2A/EBNA3A B cells, but did not elevate PC differentiation (Fig. 7D–F and *SI Appendix, Fig. S7A–C*). In iLMP1\_2A B cells, *Myc* overexpression had little impact on proliferation and differentiation. To determine the impact of *Myc* activation on iLMP1\_2A/EBNA3A B cell transformation, we transplanted  $5 \times 10^6$  *Myc*-transduced iLMP1\_2A/EBNA3A B cells into *Rag2<sup>KO</sup>cγ<sup>KO</sup>* mice. Within 90 d roughly one-third of transplanted mice developed LMP1\_2A<sup>+</sup>, EBNA3A<sup>+</sup>, and RV-*Myc*<sup>+</sup> lymphomas in spleen and liver (Fig. 7G and H). Tumors

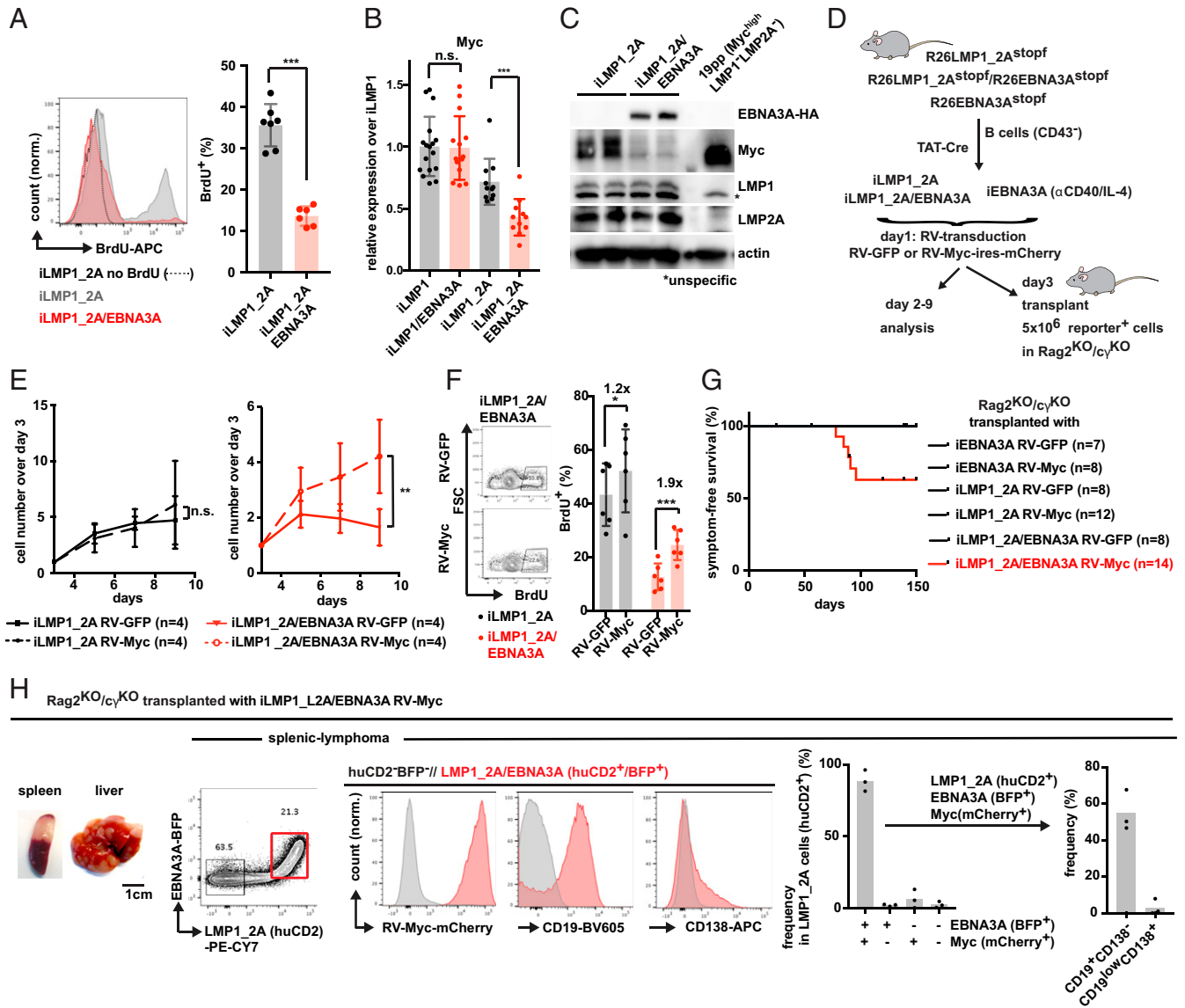


**Fig. 7.** Transformation of LMP1\_2A B cells requires overexpression of EBNA3A and Myc. (A–H) Analysis of iEBNA3A, iLMP1, iLMP1\_2A, and iLMP1\_2A/EBNA3A B cells. (A) Representative FACS analysis and quantification of BrdU incorporation day 6 post TAT-Cre;  $n = 7$  (iLMP1\_2A),  $n = 6$  (iLMP1\_2A/EBNA3A). (B) RT-qPCR-based quantification of *Myc* expression day 6 post TAT-Cre;  $n = 17$  (iLMP1),  $n = 14$  (iLMP1/EBNA3A),  $n = 11$  (iLMP1\_2A and iLMP1\_2A/EBNA3A). (C) Western blot of total cell lysates day 6 post TAT-Cre. *Myc<sup>high</sup> LMP1<sup>-</sup> LMP2A<sup>-</sup>* mouse cell line 19pp serves as expression control (80). (D) Experimental overview of *E–H*. iEBNA3A cells were stimulated with  $\alpha$ CD40 (2  $\mu$ g/mL) and IL-4 (20 ng/mL) to allow transduction. (E) Growth curve of transduced (GFP<sup>+</sup> or mCherry<sup>+</sup>) cells in bulk. (F) Representative FACS analysis and quantification of BrdU uptake on day 6 post TAT-Cre;  $n = 6$ . (G and H) Analysis of *Rag2<sup>KO</sup>cγ<sup>KO</sup>* mice transplanted with  $5 \times 10^6$  transduced cells; three independent donors per group. (G) Survival curve. (H) Representative organ images and FACS analysis of mice transplanted with RV-*Myc* transduced iLMP1\_2A/EBNA3A B cells at disease onset. Quantifications show BFP/mCherry expression in huCD2<sup>+</sup> cells and CD19/CD138 expression on huCD2<sup>+</sup>/BFP<sup>+</sup>/mCherry<sup>+</sup> cells.  $n = 3$ . All data are presented as mean  $\pm$  SD. Significance was calculated using a Student's *t* test (A), Mann-Whitney *U* test (B), or paired Student's *t* test (E and F). (\**P* < 0.05; \*\**P* < 0.005; \*\*\**P* < 0.0005; n.s., nonsignificant).

were clonal, as indicated by VDJ-diversity restriction (*SI Appendix, Fig. S7D*) and expressed CD19 but not CD138 (*Fig. 7H*), suggesting that blocked PC differentiation is also important in such lymphomas. *Rag2<sup>KO</sup>cy<sup>KO</sup>* mice transplanted with control cells, including *Myc*-transduced iLMP1\_2A B cells, did not develop lymphomas within the observation period of 150 d (*Fig. 7G*). Thus, aberrant *Myc* activation overrides EBNA3A-suppressive effects on proliferation and together with EBNA3A allows transformation of LMP1\_2A B cells in vivo.

## Discussion

Here we investigate interlocking functions of EBV genes during EBV-driven B cell lymphomagenesis. We had previously shown that expression of LMP1 in mouse B cells causes spontaneous LMP1-L development in T cell-deficient mice (20). We now find that all LMP1-Ls aberrantly activate either *Ebf1* or *Rel* either by translocation into the Ig locus or other unknown mechanisms, which possibly include the recurrent amplification of the *Ebf1*- and *Rel*-encoding chromosome 11. Overexpression of either gene with LMP1 in mouse B cells efficiently facilitates their transformation in vitro and in vivo, arguing that *Ebf1* and *Rel* are potent oncogenes in LMP1-driven B cells. The finding that LMP1/EBF1-expressing B cells can grow out from single cells even suggests that this oncogene combination does not depend on additional mutations to transform at least a subset of B cells. Indeed, the frequency in which LMP1/EBF1 coexpression transforms single-sorted mouse B cells in vitro (~2%) is similar to the transforming efficiency of EBV in human B cells (~3 to 10%) (1, 44). Thus, coexpression of a single viral and a single somatic gene recapitulates EBV-mediated transformation of B cells in vitro and in vivo and underlines the transforming potential of EBV oncoprotein LMP1. Indeed, B cell transformation driven by *MYC*, considered to be one of the most potent oncogenes in B cells, still requires overexpression of at least two additional factors, like *BCL6/BCL2* or *BMI1/BCLXL* or *BMI1/MCL1* (27, 45). In the future, mouse EBF1-LCLs might serve, like their human counterparts, as a simple and powerful tool for in vitro expansion of mature B cells, independent of exogenous cytokines or feeders.

Given their potential to transform LMP1 B cells, we considered EBF1 and c-Rel as possible surrogates for EBV proteins that would cooperate with LMP1 in EBV-driven B cell transformation. The distinct gene expression patterns of *Ebf1<sup>high</sup>* and *Rel<sup>high</sup>* LMP1-Ls might reflect different modes of viral lymphomagenesis. Importantly, EBF1 and to a minor extent c-Rel also supported the expansion of LMP1-expressing human GCBs, indicating that the presented mouse model can predict genes that synergize with LMP1 in the transformation of human B cells.

*REL* is frequently amplified in human B cell lymphomas especially GCB-DLBCLs and HL, suggesting an important oncogenic role (46). Yet, no direct evidence for c-Rel oncogenicity in a mouse B cell lymphoma model has, to our knowledge, been reported. On the contrary, c-Rel was shown to be a tumor suppressor in *EμMyc* lymphomas (47). We now find *Rel* to be a potent oncogene in mouse LMP1 B cells. Aberrant *Rel* expression likely supports LMP1-driven lymphomagenesis by promoting expression of a subset of protooncogenic NF-κB targets like Bcl-X and A1/BFL-1, overcoming LMP1-mediated repression of endogenous *Rel*. Thus, transformation of mouse B cells appears to benefit from a dual activation of NF-κB. LMP1 constitutively activates the IKK signaling cascade, while *Rel* induction ensures sufficient expression of c-Rel-sensitive oncogenic targets. As *REL* is not specifically overexpressed in human EBV<sup>+</sup> PT-ABC-DLBCL over EBV<sup>-</sup> cases and not commonly amplified in EBV<sup>+</sup> DLBCL cases (35, 37, 38), we suspect that other EBV gene products substitute for *REL* overexpression during the transformation of human B cells. Possible candidates are LMP2A and viral miRNAs which have been

shown to modulate LMP1-driven NF-κB signaling (48, 49). If not in PTLs, the synergy of LMP1 and c-Rel might play out in the pathogenesis of human HLs which often carry *REL* amplifications (~20% of cases) and express LMP1<sup>+</sup> EBV latency II (~40% of cases) (50, 51). To our knowledge an analysis overlaying *REL* amplification with LMP1 expression in HL has not yet been performed.

The recurrent activation of *Ebf1* in LMP-Ls was surprising, since *Ebf1* is not considered to be an oncogene, but has rather been described as a tumor suppressor in acute lymphoblastic leukemia (52, 53). Some cases of DLBCL were reported to carry mutated, deleted, or Ig-translocated *EBF1*, but the impact of such mutations on tumorigenesis has remained elusive (36, 54–56). Interestingly, *EBF1* is among eight genes whose knockout is lethal in human ABC-DLBCL but not GCB-DLBCL cell lines (57), supporting the idea that EBF1 plays an important role specifically in ABC-DLBCLs. We find that *Ebf1* overexpression is sufficient to block cytokine- and LMP-driven PC differentiation of mouse B cells. Importantly, a loss of PC-differentiation potential was previously shown to promote ABC-DLBCL onset in humans and mice (32, 58–60). As LMP1-Ls resemble ABC-DLBCLs, EBF1 likely supports transformation of LMP1 B cells through inhibition of terminal PC differentiation.

In contrast to mouse LMP1 B cells, transformation of human B cells by EBV latency III is not known to require additional somatic mutations (1, 61). Assuming that inhibition of LMP-driven PC differentiation is indeed a critical step in the transformation of human B cells by EBV, one would predict that EBV itself encodes an inhibitor of PC differentiation. Indeed, the EBV-gene products LMP1, miR-BHRF1-2, EBNA1, and most recently EBNA3A and 3C, were reported to impact PC differentiation of EBV-infected human B cells in vitro (62–65). We now show that EBNA3A inhibits PC differentiation and promotes lymphomagenesis of mouse LMP1 B cells in vivo. (EBNA3C did not, for unknown reasons, affect mouse B cells). Overexpression of *Prdm1* was sufficient to overcome EBNA3A-suppressive effects on PC differentiation in this system. Indeed, *Prdm1* is a direct target of EBNA3A in human cells (65), supporting the idea that EBNA3A engages the same pathways in mouse and human cells. As our data predicted that EBF1 can substitute for EBNA3A in LMP-driven B cell transformation, we wondered whether *EBF1* might be selectively activated in human latency II (LMPs<sup>+</sup>EBNA3A<sup>-</sup>) PTLs. Yet, *EBF1* expression in human PT-ABC-DLBCL was rather reduced in latency II over latency III cases. While this was surprising, the low case number in the study might be insufficient to detect rare *EBF1<sup>high</sup>* tumors. Note that in our mouse model only a subset of tumors is driven by EBF1. The low *EBF1* expression in latency II tumors might also reflect that the progenitor cells of such lymphomas expressed the EBV latency III program, including EBNA3 expression, as this is the default EBV program after initial B cell infection (1). If EBNA3 expression epigenetically silences *PRDM1* at this stage as it does in human LCLs (65), this would render the malignant progeny independent of EBF1 activation, even after a switch to latency II. Taken together, our findings indicate that shared regulation of PC differentiation is critical for EBF1's and EBNA3A's oncogenic activity. Still, the two proteins likely have additional nonshared functions during transformation. In the case of EBNA3A, one such activity might be the observed suppression of *Cdkn2a* and *Bcl2l11*. Although knockout of either gene was insufficient to promote the expansion of LMP1 B cells, their coregulation might still serve this purpose, an issue that remains to be addressed.

Coexpression of LMP1 and LMP2A, as observed in the EBV growth program, promoted B cell expansion and PC differentiation, but transformation was still restricted to cells that did not undergo PC differentiation. Although EBNA3A suppressed differentiation and supported survival of LMP1/2A expressing

B cells, it did not promote their transformation, but blunted their proliferation through the inhibition of *Myc* transcription. This is in line with reports that EBNA3A overexpression inhibits proliferation of human LCLs by silencing EBNA2-driven *MYC* transcription (43), likely through the binding EBNA3A to multiple *MYC*-enhancer sites (66). As one would then predict, overexpression of *Myc* in LMP1<sub>2A</sub>/EBNA3A mouse B cells mitigated the repressive effects of EBNA3A and allowed their transformation to lymphomas in vivo. This dependence on *Myc* activation strikingly resembles the dependence of EBV-driven B cell transformation on the *MYC* activator EBNA2 (67). Importantly, transplantation of LMP1, LMP2A, EBNA3A, and *Myc* coexpressing B cells caused clonal lymphomagenesis, arguing that transformation of such cells still depends on secondary events. Defining such secondary events along the lines of the present analysis might shed light on additional functions of other EBV genes during the transformation of human B cells. Unexpectedly, EBNA3A did not impact *Myc* transcription in LMP1-only B cells. This might be due to elevated expression of LMP1 from the *R26LMP1* over the *R26LMP1t2aLMP2A* allele. More likely, and consistent with the highly cell type-, signaling- and EBV-dependent selection of *Myc* enhancers (68–72), integrated LMP1 and LMP2A signaling engages *Myc* enhancers distinct from those used in LMP1-only B cells and more sensitive to EBNA3A. Such differential use of *Myc* enhancers should be addressed in future studies, albeit in human B cells.

In summary, our conditional EBV-transgenic mice represent a system to study interlocking functions of viral oncogenes in B cell lymphomagenesis. The presented data reveal a model of EBV-driven B cell lymphomagenesis in which LMPs induce B cell proliferation but also promote differentiation to non-transforming PCs. EBNA3A blocks PC differentiation but simultaneously inhibits *Myc*-driven proliferation. This inhibition

does not play out in the presence of the EBV *MYC*-activator EBNA2, allowing B cell transformation.

## Methods

**Mouse Strains and Handling.** *Cd19-Cre* (73), *Cy1-Cre* (74), *Rosa26LMP1<sup>stopf</sup>* (21), *Rosa26LMP2A<sup>stopf</sup>* (41), *Rosa26Cas9<sup>tg</sup>* (75), *Rag2<sup>KO</sup>* (76), *Il2rg<sup>KO</sup>* (*Cy<sup>KO</sup>*) (77), and *Cd3ε<sup>KO</sup>* (78) mouse strains were described before. Unless noted, mice were used between 8 and 30 wk of age and indiscriminately of their sex. *Cre* and *R26* alleles were always heterozygous. Animals developing pathologies did not succumb to the disease but were killed once defined humane termination criteria were reached. Animal procedures were approved by the Landesamt für Gesundheit und Soziales Berlin (G0049/15, G0374/13, and G0135/11).

**Data Presentation and Statistical Analysis.** Unless noted otherwise, single dots or indicated n-values represent number of biological replicates from independent mice or human donors. Unless noted otherwise, bars represent mean ± SD. Two-sided tests for significance were chosen by assumed data distribution and variation and are noted in the figure legends. When noted, *P* values were adjusted for multiple testing.

**Data Availability.** RNA sequencing, exome sequencing, and array CGH data are available at the GEO repository under the accession no. GSE136075 (79).

Further methods and critical reagents can be found in [SI Appendix](#).

**ACKNOWLEDGMENTS.** We thank all members of the K.R. laboratory for assistance and discussion. We thank the Genomics, Transgenics, and Flow Cytometry core facilities at the Max Delbrück Center for Molecular Medicine as well as F. Lasitschka, R. Rad, and N. Gross for technical assistance. We thank M. Janz, W. Hammerschmidt, E. Kieff, B. Gewurz, and B. Zhao for sharing materials. This work was supported by the European Research Council Advanced Grant 268921 to K.R. and by the “Helmholtz Alliance Preclinical Comprehensive Cancer Center” of the Helmholtz Association’s Initiative and Networking Fund (HA-305) and by the Helmholtz-Gemeinschaft, Zukunftsthema “Immunology and Inflammation” (ZT-0027). R.C. and D.J.H. were supported by the Medical Research Council, UK.

- L. S. Young, L. F. Yap, P. G. Murray, Epstein-Barr virus: More than 50 years old and still providing surprises. *Nat. Rev. Cancer* **16**, 789–802 (2016).
- G. S. Taylor, H. M. Long, J. M. Brooks, A. B. Rickinson, A. D. Hislop, The immunology of Epstein-Barr virus-induced disease. *Annu. Rev. Immunol.* **33**, 787–821 (2015).
- S. H. Swerdlow, S. A. Webber, A. Chadburn, J. A. Ferry, “Post-transplant lymphoproliferative disorders” in *WHO Classification of Tumours of Haematopoietic and Lymphoid Tissues*, (International Agency for Research on Cancer, ed. 4, 2008), pp. 343–349.
- J. Morscio, T. Tousseyn, Recent insights in the pathogenesis of post-transplantation lymphoproliferative disorders. *World J. Transplant.* **6**, 505–516 (2016).
- A. Kieser, K. R. Sterz, “The latent membrane protein 1 (LMP1)” in *Curr. Top. Microbiol. Immunol.*, (2015), Vol. 391, pp. 119–149.
- J. Rastelli et al., LMP1 signaling can replace CD40 signaling in B cells in vivo and has unique features of inducing class-switch recombination to IgG1. *Blood* **111**, 1448–1455 (2008).
- O. Cen, R. Longnecker, “Latent membrane protein 2 (LMP2)” in *Curr. Top. Microbiol. Immunol.*, (2015), Vol. 391, pp. 151–180.
- R. G. Caldwell, J. B. Wilson, S. J. Anderson, R. Longnecker, Epstein-Barr virus LMP2A drives B cell development and survival in the absence of normal B cell receptor signals. *Immunity* **9**, 405–411 (1998).
- S. Casola et al., B cell receptor signal strength determines B cell fate. *Nat. Immunol.* **5**, 317–327 (2004).
- B. Kempkes, P. D. Ling, “EBNA2 and its coactivator EBNA-LP” in *Curr. Top. Microbiol. Immunol.*, (2015), Vol. 391, pp. 35–59.
- M. J. Allday, Q. Bazot, R. E. White, “The EBNA3 family: Two oncoproteins and a tumour suppressor that are central to the biology of EBV in B cells” in *Curr. Top. Microbiol. Immunol.*, (2015), Vol. 391, pp. 61–117.
- F. Wang, Nonhuman primate models for Epstein-Barr virus infection. *Curr. Opin. Virol.* **3**, 233–237 (2013).
- J. Törnell et al., Expression of Epstein-Barr nuclear antigen 2 in kidney tubule cells induce tumors in transgenic mice. *Oncogene* **12**, 1521–1528 (1996).
- D. S. Huen, A. Fox, P. Kumar, P. F. Searle, Dilated heart failure in transgenic mice expressing the Epstein-Barr virus nuclear antigen-leader protein. *J. Gen. Virol.* **74**, 1381–1391 (1993).
- R. G. Caldwell, R. C. Brown, R. Longnecker, Epstein-Barr virus LMP2A-induced B-cell survival in two unique classes of EmuLMP2A transgenic mice. *J. Virol.* **74**, 1101–1113 (2000).
- M.-S. Kang et al., Epstein-Barr virus nuclear antigen 1 does not induce lymphoma in transgenic FVB mice. *Proc. Natl. Acad. Sci. U.S.A.* **102**, 820–825 (2005).
- J. B. Wilson, J. L. Bell, A. J. Levine, Expression of Epstein-Barr virus nuclear antigen-1 induces B cell neoplasia in transgenic mice. *EMBO J.* **15**, 3117–3126 (1996).
- W. Kulwicht et al., Expression of the Epstein-Barr virus latent membrane protein 1 induces B cell lymphoma in transgenic mice. *Proc. Natl. Acad. Sci. U.S.A.* **95**, 11963–11968 (1998).
- C. Münz, Humanized mouse models for Epstein Barr virus infection. *Curr. Opin. Virol.* **25**, 113–118 (2017).
- B. Zhang et al., Immune surveillance and therapy of lymphomas driven by Epstein-Barr virus protein LMP1 in a mouse model. *Cell* **148**, 739–751 (2012).
- T. Yasuda et al., Studying Epstein-Barr virus pathologies and immune surveillance by reconstructing EBV infection in mice. *Cold Spring Harb. Symp. Quant. Biol.* **78**, 259–263 (2013).
- C. P. Hans et al., Confirmation of the molecular classification of diffuse large B-cell lymphoma by immunohistochemistry using a tissue microarray. *Blood* **103**, 275–282 (2004).
- J. C. Strefford, Q. An, C. J. Harrison, Modeling the molecular consequences of unbalanced translocations in cancer: Lessons from acute lymphoblastic leukemia. *Cell Cycle* **8**, 2175–2184 (2009).
- R. Küppers, Mechanisms of B-cell lymphoma pathogenesis. *Nat. Rev. Cancer* **5**, 251–262 (2005).
- J. M. Wroblewski, A. Copple, L. P. Batson, C. D. Landers, J. R. Yannelli, Cell surface phenotyping and cytokine production of Epstein-Barr Virus (EBV)-transformed lymphoblastoid cell lines (LCLs). *J. Immunol. Methods* **264**, 19–28 (2002).
- E. D. Cahir-McFarland et al., Role of NF-κB in cell survival and transcription of latent membrane protein 1-expressing or Epstein-Barr virus latency III-infected cells. *J. Virol.* **78**, 4108–4119 (2004).
- R. Caesar et al., Genetic modification of primary human B cells to model high-grade lymphoma. *Nat. Commun.* **10**, 4543 (2019).
- R. Nechanitzky et al., Transcription factor EBF1 is essential for the maintenance of B cell identity and prevention of alternative fates in committed cells. *Nat. Immunol.* **14**, 867–875 (2013).
- W. Shi et al., Transcriptional profiling of mouse B cell terminal differentiation defines a signature for antibody-secreting plasma cells. *Nat. Immunol.* **16**, 663–673 (2015).
- T. Nojima et al., In-vitro derived germinal centre B cells differentially generate memory B or plasma cells in vivo. *Nat. Commun.* **2**, 465 (2011).
- K. Roy et al., A regulatory circuit controlling the dynamics of NFκB cRel transitions B cells from proliferation to plasma cell differentiation. *Immunity* **50**, 616–628.e6 (2019).
- D. P. Calado et al., Constitutive canonical NF-κB activation cooperates with disruption of BLIMP1 in the pathogenesis of activated B cell-like diffuse large cell lymphoma. *Cancer Cell* **18**, 580–589 (2010).
- M. Swanson-Mungerson, R. Bultema, R. Longnecker, Epstein-Barr virus LMP2A enhances B-cell responses in vivo and in vitro. *J. Virol.* **80**, 6764–6770 (2006).

34. J. Morscio *et al.*, Gene expression profiling reveals clear differences between EBV-positive and EBV-negative posttransplant lymphoproliferative disorders. *Am. J. Transplant.* **13**, 1305–1316 (2013).
35. J. F. Ferreira *et al.*, EBV-positive and EBV-negative posttransplant diffuse large B cell lymphomas have distinct genomic and transcriptomic features. *Am. J. Transplant.* **16**, 414–425 (2016).
36. T. Menter *et al.*, Mutational landscape of B-cell post-transplant lymphoproliferative disorders. *Br. J. Haematol.* **178**, 48–56 (2017).
37. A. Rinaldi *et al.*, Single nucleotide polymorphism-arrays provide new insights in the pathogenesis of post-transplant diffuse large B-cell lymphoma. *Br. J. Haematol.* **149**, 569–577 (2010).
38. H. A. Poirel *et al.*, Characteristic pattern of chromosomal imbalances in post-transplantation lymphoproliferative disorders: Correlation with histopathological subcategories and EBV status. *Transplantation* **80**, 176–184 (2005).
39. E. Vakiani *et al.*, Genetic and phenotypic analysis of B-cell post-transplant lymphoproliferative disorders provides insights into disease biology. *Hematol. Oncol.* **26**, 199–211 (2008).
40. F. E. Craig *et al.*, Gene expression profiling of Epstein-Barr virus-positive and -negative monomorphic B-cell posttransplant lymphoproliferative disorders. *Diagn. Mol. Pathol.* **16**, 158–168 (2007).
41. T. Wirtz *et al.*, Mouse model for acute Epstein-Barr virus infection. *Proc. Natl. Acad. Sci. U.S.A.* **113**, 13821–13826 (2016).
42. T. Minamitani *et al.*, Mouse model of Epstein-Barr virus LMP1- and LMP2A-driven germinal center B-cell lymphoproliferative disease. *Proc. Natl. Acad. Sci. U.S.A.* **114**, 4751–4756 (2017).
43. A. Cooper *et al.*, EBNA3A association with RBP-Jkappa down-regulates c-myc and Epstein-Barr virus-transformed lymphoblast growth. *J. Virol.* **77**, 999–1010 (2003).
44. C. Shannon-Lowe *et al.*, Epstein-Barr virus-induced B-cell transformation: Quantitating events from virus binding to cell outgrowth. *J. Gen. Virol.* **86**, 3009–3019 (2005).
45. K. Höglstrand, A. Grandien, MYC-driven malignant transformation of mature murine B cells requires inhibition of both intrinsic apoptosis and p53 activity. *Eur. J. Immunol.* **49**, 375–385 (2019).
46. J. E. Hunter, J. Leslie, N. D. Perkins, c-Rel and its many roles in cancer: An old story with new twists. *Br. J. Cancer* **114**, 1–6 (2016).
47. J. E. Hunter *et al.*, The NF- $\kappa$ B subunit c-Rel regulates Bach2 tumour suppressor expression in B-cell lymphoma. *Oncogene* **35**, 3476–3484 (2016).
48. Y. Chen, D. Fachko, N. S. Ivanov, C. M. Skinner, R. L. Skalsky, Epstein-Barr virus microRNAs regulate B cell receptor signal transduction and lytic reactivation. *PLoS Pathog.* **15**, e1007535 (2019).
49. I. Guasparri, D. Bubman, E. Cesarman, EBV LMP2A affects LMP1-mediated NF-kappaB signaling and survival of lymphoma cells by regulating TRAF2 expression. *Blood* **111**, 3813–3820 (2008).
50. J. I. Martín-Subero *et al.*, Recurrent involvement of the REL and BCL11A loci in classical Hodgkin lymphoma. *Blood* **99**, 1474–1477 (2002).
51. R. Küppers, A. Engert, M.-L. Hansmann, Hodgkin lymphoma. *J. Clin. Invest.* **122**, 3439–3447 (2012).
52. C. G. Mullighan *et al.*, Genome-wide analysis of genetic alterations in acute lymphoblastic leukaemia. *Nature* **446**, 758–764 (2007).
53. E. Tijchon, J. Havinga, F. N. van Leeuwen, B. Scheijen, B-lineage transcription factors and cooperating gene lesions required for leukemia development. *Leukemia* **27**, 541–552 (2013).
54. H. Bouamar *et al.*, A capture-sequencing strategy identifies IRF8, EBF1, and APRIL as novel IGH fusion partners in B-cell lymphoma. *Blood* **122**, 726–733 (2013).
55. K. Karube *et al.*, Integrating genomic alterations in diffuse large B-cell lymphoma identifies new relevant pathways and potential therapeutic targets. *Leukemia* **32**, 675–684 (2018).
56. R. Schmitz *et al.*, Genetics and pathogenesis of diffuse large B-cell lymphoma. *N. Engl. J. Med.* **378**, 1396–1407 (2018).
57. A. Reddy *et al.*, Genetic and functional drivers of diffuse large B cell lymphoma. *Cell* **171**, 481–494.e15 (2017).
58. W. Tam *et al.*, Mutational analysis of PRDM1 indicates a tumor-suppressor role in diffuse large B-cell lymphomas. *Blood* **107**, 4090–4100 (2006).
59. L. Pasqualucci *et al.*, Inactivation of the PRDM1/BLIMP1 gene in diffuse large B cell lymphoma. *J. Exp. Med.* **203**, 311–317 (2006).
60. J. Mandelbaum *et al.*, BLIMP1 is a tumor suppressor gene frequently disrupted in activated B cell-like diffuse large B cell lymphoma. *Cancer Cell* **18**, 568–579 (2010).
61. R. Küppers, B cells under influence: transformation of B cells by Epstein-Barr virus. *Nat. Rev. Immunol.* **3**, 801–812 (2003).
62. A. Onnis *et al.*, Epstein-Barr nuclear antigen 1 induces expression of the cellular microRNA hsa-miR-127 and impairing B-cell differentiation in EBV-infected memory B cells. New insights into the pathogenesis of Burkitt lymphoma. *Blood Cancer J.* **2**, e84 (2012).
63. J. Ma *et al.*, EBV-miR-BHRF1-2 targets PRDM1/Blimp1: Potential role in EBV lymphomagenesis. *Leukemia* **30**, 594–604 (2016).
64. K. Vrzalikova *et al.*, Down-regulation of BLIMP1 $\alpha$  by the EBV oncogene, LMP-1, disrupts the plasma cell differentiation program and prevents viral replication in B cells: Implications for the pathogenesis of EBV-associated B-cell lymphomas. *Blood* **117**, 5907–5917 (2011).
65. C. T. Styles *et al.*, EBV epigenetically suppresses the B cell-to-plasma cell differentiation pathway while establishing long-term latency. *PLoS Biol.* **15**, e2001992 (2017).
66. S. C. S. Schmidt *et al.*, Epstein-Barr virus nuclear antigen 3A partially coincides with EBNA3C genome-wide and is tethered to DNA through BATF complexes. *Proc. Natl. Acad. Sci. U.S.A.* **112**, 554–559 (2015).
67. J. I. Cohen, F. Wang, J. Mannick, E. Kieff, Epstein-Barr virus nuclear protein 2 is a key determinant of lymphocyte transformation. *Proc. Natl. Acad. Sci. U.S.A.* **86**, 9558–9562 (1989).
68. J. Schuijers *et al.*, Transcriptional dysregulation of MYC reveals common enhancer-docking mechanism. *Cell Rep.* **23**, 349–360 (2018).
69. C. Bahr *et al.*, A Myc enhancer cluster regulates normal and leukaemic haematopoietic stem cell hierarchies. *Nature* **553**, 515–520 (2018).
70. D. Herranz *et al.*, A NOTCH1-driven MYC enhancer promotes T cell development, transformation and acute lymphoblastic leukemia. *Nat. Med.* **20**, 1130–1137 (2014).
71. S. Jiang *et al.*, The Epstein-Barr virus regulome in lymphoblastoid cells. *Cell Host Microbe* **22**, 561–573.e4 (2017).
72. H. Zhou *et al.*, Epstein-Barr virus oncoprotein super-enhancers control B cell growth. *Cell Host Microbe* **17**, 205–216 (2015).
73. R. C. Rickert, J. Roes, K. Rajewsky, B lymphocyte-specific, Cre-mediated mutagenesis in mice. *Nucleic Acids Res.* **25**, 1317–1318 (1997).
74. S. Casola *et al.*, Tracking germinal center B cells expressing germ-line immunoglobulin gamma1 transcripts by conditional gene targeting. *Proc. Natl. Acad. Sci. U.S.A.* **103**, 7396–7401 (2006). Correction in: *Proc. Natl. Acad. Sci. U.S.A.* **104**, 2025 (2007).
75. V. T. Chu *et al.*, Efficient generation of Rosa26 knock-in mice using CRISPR/Cas9 in C57BL/6 zygotes. *BMC Biotechnol.* **16**, 4 (2016).
76. Z. Hao, K. Rajewsky, Homeostasis of peripheral B cells in the absence of B cell influx from the bone marrow. *J. Exp. Med.* **194**, 1151–1164 (2001).
77. J. P. DiSanto, W. Müller, D. Guy-Grand, A. Fischer, K. Rajewsky, Lymphoid development in mice with a targeted deletion of the interleukin 2 receptor gamma chain. *Proc. Natl. Acad. Sci. U.S.A.* **92**, 377–381 (1995).
78. M. Malissen *et al.*, Altered T cell development in mice with a targeted mutation of the CD3-epsilon gene. *EMBO J.* **14**, 4641–4653 (1995).
79. T. Sommermann *et al.*, Functional interplay of Epstein-Barr Virus oncoproteins in a mouse model of B cell lymphomagenesis. Gene Expression Omnibus. <https://www.ncbi.nlm.nih.gov/geo/query/acc.cgi?acc=GSE136075>. Deposited 20 August 2019.
80. Sandrine Sander *et al.*, Synergy between PI3K signaling and MYC in Burkitt lymphomagenesis. *Cancer Cell* **22** (2), 167–179, 10.1016/j.ccr.2012.06.012 (2012).